Solid-State Electronics Vol. 24, pp. 69–78
Pergamon Press Ltd., 1981. Printed in Great Britain

LOW RESISTANCE OHMIC CONTACTS TO *n*- AND *p*-InP

E. KUPHAL
Forschungsinstitut der Deutschen Bundespost beim FTZ, D-6100 Darmstadt, Federal Republic of Germany

(*Received* 23 *February* 1980; *in revised form* 9 *June* 1980)

Abstract—The contact properties of various metal combinations, deposited by vacuum evaporation on InP, were studied. Among these metal combinations, Au/Ge + Ni and Au/Zn proved to be most suitable. The former on *n*-InP ($n = 8 \times 10^{17}/cm^3$) and the latter on *p*-InP ($p = 9 \times 10^{17}/cm^3$) exhibited specific contact resistances as low as 1.2×10^{-6} and $1.1 \times 10^{-4}\,\Omega cm^2$, respectively. The specific contact resistances were analyzed using a four-point method which also accounts for the spreading resistance. Furthermore, the resistances of metal contacts to InP were calculated as a function of doping concentration and were compared with the experimental results. The described contacting technique was successfully applied to the preparation of quaternary lasers.

1. INTRODUCTION

Ohmic contacts to InP with low specific contact resistance are especially required for $InP/In_{1-x}Ga_xP_{1-y}As_y$ laser diodes because of the high current density used in these devices. A realistic threshold current density of $4\,kA/cm^2$ in narrow stripe quaternary lasers combined with typical specific contact resistances $\rho_c(n^+\text{-InP}) = 10^{-4}\,\Omega cm^2$ and $\rho_c(p^+\text{-InP}) = 10^{-3}\,\Omega cm^2$ yields a voltage drop of 0.4 V and 4 V at the n^+- and p^+-InP contacts, respectively. As the voltage drop in the *p*–*n*-heterojunction is only ≈1 V, most of the power of the device is consumed in the *p*-contact.

In Table 1 published data on ohmic contacts to *n*-InP are collected. Becker[1] achieved ohmic contacts with In and Sn. However, these metals showed the tendency of island formation during the heat treatment. The island formation was avoided in the system In/Sn/Ag[2] by the deposition of an Ag layer several microns in thickness. Such contacts cannot be defined by the conventional lift-off technique and are, therefore, less suitable for device applications. In/Sn/Ag contacts, which were heat treated in a closed ampoule under over-pressure of phosphorus[3], showed very smooth surfaces. The latter technique is, however, more complicated. The lowest ρ_c-values were obtained so far with the system Au/Ge/Ni and with Ni[4]. Table 1 also quotes a selection of publications on InP devices, in which the ohmic contact technology is mentioned. In the majority of the studies, Au/Sn contacts were employed, but in no case a ρ_c-value is quoted.

In Table 2 published data on ohmic contacts to *p*-InP are compiled. The lowest ρ_c-value was obtained with Au/Mg to be $\sim 1 \times 10^{-4}\,\Omega cm^2$[4]. In addition, some papers on InP devices are cited, where also the ohmic contact technology is described. Mostly, Au/Zn contacts were employed, but it is not evident, whether these metals were sequentially evaporated or evaporated from an alloy. Although in no case ρ_c-values were reported, it can be derived from the differential resistance of laser diodes in some studies that $\rho_c < 10^{-3}\,\Omega cm^2$ was achieved.

It was the aim of this study to fabricate mechanically reliable ohmic contacts for lasers by vacuum deposition, which show a low contact resistance, a smooth surface, and a good lift-off behaviour during photolithography.

2. THEORETICAL ESTIMATE OF THE CONTACT RESISTANCE

2.1 *Barrier height of InP surfaces*

Metal contacts to semiconductors with not too small an energy gap E_g always show a rectifying characteristic at room temperature, which is due to the surface Schottky barrier. For many covalent semiconductors, Mead[12] has established the rule that the barrier height ϕ_{BO} of *n*-type semiconductors equals 2/3 E_g and that of *p*-type semiconductors equals 1/3 E_g. This means that ϕ_{BO} is essentially independent of the work function of the used metal. This is commonly interpreted in terms of Fermi pinning at the semiconductor surface due to the high density N_{ss} of surface states. Mead's rule has particularly been proved for GaAs[12]. It is consistent with the finding that real GaAs surfaces show a high N_{ss}. The energy distribution of N_{ss} is parabola-like with an increase at the band edges and a minimum in the middle of the bandgap[13]. InP is an exception to Mead's rule, since ϕ_{BO}, as measured in Schottky diodes, is only 0.48 eV for the metals Au, Al or Ti on *n*-InP[14, 15], but $\phi_{BO} \geq 0.75$ eV for Au on *p*-InP[15]. The energy distribution of N_{ss} in InP is also parabola-like; however, its minimum is positioned near the conduction band edge[16] and it increases towards the valence band edge. As a consequence, the surface of *n*-InP is only slightly depleted. This result is consistent with the measured low ϕ_{BO} of *n*-InP and high ϕ_{BO} of *p*-InP. Therefore, it should be possible to realize very low resistance ohmic contacts to *n*-InP by alloying. On the other hand, for *p*-InP an increased contact resistance is expected.

2.2 *Resistance of metal-InP contacts*

The electrical properties of a metal-semiconductor contact depend on the height ϕ_{BO} of the surface barrier, the density N of ionized dopant atoms near the surface,

Table 1. Published data on ohmic contacts to *n*-InP

InP n/cm^{-3}	Contacting technique		Alloying t/min	Alloying T/°C	$\rho_c/\Omega cm^2$	Application	Reference
3×10^{15}	In Sn	Evapor. "	0.05...1	200 ... 450	ohmic		[1]
1×10^{18}	In/Sn/Ag	"	2	350, in H_2	1.3×10^{-4}		[2]
$\sim 2 \times 10^{15}$	Sn/Ag	"	5	470, in H_2	2×10^{-3}		[3]
	In/Sn/Ag	"		470	$<10^{-4}$	Gunn diodes	[3]
3×10^{16}	Ge/Au/Ni	"	5	325, in N_2	3×10^{-5}		[4]
3×10^{16}	Ni	"	5	325, in N_2	4×10^{-5}		[4]
3×10^{18}	Au/Sn	"		350		Laser on p-type substrate	[5]
n^+	Sn/Ni/Au	Plating		350, in forming gas		LED	[6]
n^+	Au/Sn	Plating		400, in N_2		Photodiode	[7]
n^+	Au/Sn/Te	Evapor.	2	400		Photodiode	[8]
2×10^{18}	Au/Sn	"	3	400, in forming gas		CW-Laser	[9]

Table 2. Published data on ohmic contacts to *p*-InP

InP p/cm^{-3}	Contacting technique		Alloying t/min	Alloying T/°C	$\rho_c/\Omega cm^2$	Application	Reference
$\sim 5 \times 10^{16}$	Au/Zn/Au	Plating	0.25	475, in forming gas	$<10^{-3}$		[10]
5×10^{16}	In	Ball contacts	5	400 - 450	non-linear		[11]
5×10^{16}	In/Cd	" "	5	400 - 450	non-linear		[11]
5×10^{16}	Au/Cd	" "	5	400 - 450	$<10^{-2}$		[11]
5×10^{16}	In/Zn	" "	5	400 - 450	2×10^{-2}		[11]
5×10^{16}	Au/Zn	" "	5	400 - 450	1×10^{-2}		[11]
1×10^{18}	In/Zn/Ag/Au	Evaporated	10	400	3×10^{-3}		[2]
6×10^{17}	Mg/Au	"	50	446, in N_2	$\sim 1 \times 10^{-4}$		[4]
4×10^{18}	Au/Zn	"		350		Laser on p-type substrate	[5]
p^+	Zn/Au	Plating		350, in forming gas		LED	[6]
p^+	Au/Mg	Evaporated		400, in N_2		Photodiode	[7]
1×10^{18}	Au/Zn	"	3	400, in forming gas		CW-Laser	[9]

the effective mass m^* of the majority carriers and the static permittivity ϵ_s of the semiconductor. There are three types of conduction mechanisms through a metal-semiconductor contact: (1) Thermionic emission of carriers over the barrier; (2) thermionic field emission (*T–F*-emission) and (3) pure field emission through the barrier[17].

Thermionic emission dominates, if N is small. The specific contact resistance for zero bias for this type of carrier transport is derived from Schottky's diode equation as

$$\rho_c{}^I = \frac{k}{eA^*T}\exp(\phi_B/kT), \tag{1}$$

where

$$A^* = \frac{m^*}{m_0}120\frac{A}{\mathrm{cm}^2K^2}. \tag{2}$$

Here, k is Boltzmann's constant, A^* is the effective Richardson constant for the majority carriers, e the electronic charge, T the absolute temperature and m_0 the electronic mass. Equation (1) is independent of N and of the ideality factor of the Schottky diode.

Thermionic field emission is the tunneling of thermally excited carriers through the barrier. This process dominates for intermediate to high values of N. The corresponding specific contact resistance for zero bias is[18]

$$\rho_c{}^{II} = \frac{k}{eA^*T}\frac{\cosh\theta}{2\sqrt{(\pi\theta\tanh\theta)}}\sqrt{\left(\frac{kT}{\phi_B+\phi_F}\right)} \times\exp\left\{\frac{1}{kT}\left[-\phi_F+(\phi_F+\phi_B)\frac{\tanh\theta}{\theta}\right]\right\} \tag{3}$$

with the dimensionless parameter

$$\theta = \frac{e\hbar}{2kT}\sqrt{\left(\frac{N}{\epsilon_s\epsilon_0 m^*}\right)}. \tag{4}$$

Here, ϕ_F is the semiconductor Fermi energy, negative when in the bandgap, ϕ_B is the image-force lowered barrier height[18], h is Planck's constant, and ϵ_0 the permittivity of vacuum. The employed barrier shape is that derived from a constant dopant concentration profile, multiplied by the ratio ϕ_B/ϕ_{BO}.

Field emission dominates for very large values of N, since the barrier width is narrowed ($\sim N^{-1/2}$) and its height is lowered ($\sim -N^{1/4}$) with increasing N. The specific contact resistance for the field emission range is given by Yu[19].

From the value of θ it can be decided, which of the three processes I to 3 dominates. The validity range of eqn (3) is roughly $0.5 < \theta < 2$[18, 19]. Thermionic emission dominates if $\theta < 0.5$ (where $\tanh\theta \approx \theta$), which reduces the exponential factor of eqn (3) to $\exp(\phi_B/kT)$ in accordance with eqn (1). Field emission dominates for $\theta > 2$ (where $\tanh\theta \approx 1$) leading to an exponential dependence of ρ_c on $N^{-1/2}$. Table 3 summarizes the ranges of ionized donor concentration N_D in n-InP and acceptor concentration N_A in p-InP and the corresponding ranges of ρ_c for the three types of current transport. For p-InP only the light hole ($m^*/m_0 = 0.089$[20]) is considered because it will dominate the tunneling process due to the $\exp(-m^{*1/2})$ dependence of the tunneling probability. The discussed model further assumes that N_{ss} and therefore ϕ_{BO} is not changed by the alloying process. The heat treatment is assumed only to provide a strong doping of the semiconductor near the surface.

3. EXPERIMENTAL PROCEDURE

3.1 *Sample preparation*

The material used was Sn-doped bulk InP with a carrier concentration $n = 8\times10^{17}/\mathrm{cm}^3$, a mobility $\mu = 2010\,\mathrm{cm}^2/\mathrm{Vs}$ and a resistivity $\rho = 3.9\,\mathrm{m\Omega cm}$, and Zn-doped bulk InP with $p = 9\times10^{17}/\mathrm{cm}^3$, $\mu = 120\,\mathrm{cm}^2/\mathrm{Vs}$ and $\rho = 58\,\mathrm{m\Omega cm}$ as determined by the van der Pauw method. The (100)-oriented polished wafers, whose thickness was 270 μm, were etched in a solution of 1% Br in methanol. By standard photolithography a square

Table 3. Ranges of doping concentration and specific contact resistance using eqns (1) and (3) for the three types of current transport. Used parameters: $m^*/m_0 = 0.077$ for n-InP and 0.089 for p-InP. $\epsilon_s = 12.35$, $T = 300$ K

			Thermionic emission	T-F-emission	Field emission
	Θ		~ 0	0.5	2	$\gg 2$
n-InP	N_D/cm^{-3}	n^-	5×10^{17}	7×10^{18}	n^{++}
	Φ_B/eV	0.48	0.425	0.370	
	$\rho_c/\Omega\mathrm{cm}^2$	3.5	2.0×10^{-2}	1.5×10^{-6}	$< 10^{-6}$
p-InP	N_A/cm^{-3}	p^-	5.4×10^{17}	8.6×10^{18}	p^{++}
	Φ_B/eV	0.75	0.689	0.625	
	$\rho_c/\Omega\mathrm{cm}^2$	1.1×10^{5}	2.3×10^{2}	5.9×10^{-4}	$< 10^{-4}$

pattern of circular dots with a diameter of $d = 150\,\mu m$ and a spacing of $s = 750\,\mu m$ was produced. After the development of the photoresist the samples were further etched down by $0.2\,\mu m$ in order to improve the adhesion of the metal and to facilitate the lift-off process. The solution consisted of H_2SO_4, H_2O_2 and H_2O in the ratio 3:1:1, the etch-rate being $0.19\,\mu m$/min at 50°C. The investigated metals were deposited by thermal evaporation onto n-InP and p-InP in two separate ion-pumped vacuum systems at pressures of $<10^{-6}$ Torr. The heat treatment was performed in flowing H_2 at temperatures between 300 and 430°C during periods between 1 and 10 min. The time required to heat up and cool off the sample was 2 min each in all cases. The contacts were examined by current–voltage measurements, scanning electron microscopy and ion microprobe concentration profiling.

3.2 *Measurement of the contact resistance*

The total resistance R measured between two ohmic contacts on a conducting layer consists of the contact resistance R_c, the spreading resistance R_s under the contact, the series resistance R_m of the material between the contacts, and the resistance R_p due to probes:

$$R = R_c + R_s + R_m + R_p. \tag{5}$$

The evaluation of R_c and of the specific contact resistance $\rho_c = R_c A$, where A is the contact area, has been performed in the literature for special contact configurations. One of them is the axial geometry[21], which requires a front- and a back-side metallization of the sample. A further method, which is based on the one-dimensional transmission line model, requires a mesa-etched conducting film on a semi-insulating substrate[22]. In this study the four-point configuration according to Terry and Wilson[23] was adopted, which offers the advantage over the before mentioned methods

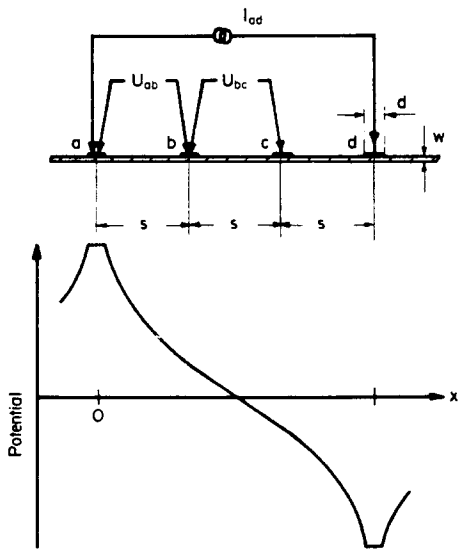

Fig. 1. Modified four-point method (on an infinite plane) to determine ρ_c (above), and approximate potential distribution on the connection line $\overline{ad}$ (below).

that only one metallization process and no mesa-etching is needed. There, 4 equidistant contacts a, b, c, d are arranged on a straight line on an infinite plane of infinitesimal thickness. The voltages U_{bc} and U'_{bc} are measured between points b, c, while the currents I_{ad} and I_{bd} are applied between points a, d and b, d, respectively. Following Ref. [23], the specific contact resistance of contact b is then

$$\rho_c = AR_c = A(R - R_m) = A\left(\frac{U'_{bc}}{I_{bd}} - \frac{U_{bc}}{I_{ad}}\right). \tag{6}$$

The resistance R_p due to probes is negligible in a high-ohmic potential measurement. However, eqn (6) contains two important simplifications: Firstly, the spreading resistance under the contact b is neglected. Secondly, the assumption is made that the series resistance R_m between points b and c is independent of the current application at a, d or b, d. This is, of course, not the case because of the logarithmic potential distribution in the layer, which is depicted in Fig. 1. Solving the two-dimensional field problem for equipotential cylinders, the potential $\varphi(x)$ on the connection line $\overline{ad}$ is

$$\varphi(x) = -\frac{I_{ad}\rho}{2\pi w}\ln\left(\frac{x}{3s - x}\right) + \varphi_0, \quad \frac{d}{2} \le x \le 3s - \frac{d}{2}, \tag{7}$$

where ρ is the resistivity, d the contact diameter, s the spacing between two neighbouring contacts and w the layer thickness. Equation (7) is valid for $d \ll s$ (i.e. no distortion of the potential by the contacts b and c) and $w \ll s$ (i.e. the current is uniform with depth). From $\varphi(x)$ the series resistance R_m outside the contacts is obtained. The spreading resistance due to planar, radial current flow under a circular contact is given by Fang *et al.*[24] to be

$$R_s = \frac{4\rho_c}{\pi d^2}\left\{\frac{\sum_{m=0}^{\infty} y^m/[2^{2m}(2m!)^2]}{\sum_{m=0}^{\infty} y^m/[(m+1)2^{2m}(m!)^2]} - 1\right\}, \tag{8}$$

where

$$y = \frac{\rho d^2}{4\rho_c w}. \tag{9}$$

For $y \le 1$, the spreading resistance is $R_s \le 0.12R_c$, which is negligible in most cases. The diameter d should be chosen such that for given ρ, ρ_c and w the value of y is not unreasonably large. Only for very thin layers the required d might be so small that the method becomes unpracticable.

The more accurate expression instead of eqn (6) is derived as

$$\rho_c = A(R - R_s - R_m) = A\left[\frac{U'_{bc}}{I_{bd}} - R_s - \frac{U_{bc}}{I_{ad}}\frac{\ln(4(s/d) - 1)}{2\ln 2}\right]. \tag{10}$$

The approximate form of Ref. [23] is only valid if $R_c \gg$

Table 4. Technological and electrical properties of various contacts to InP with a bulk carrier concentration of $n = 8 \times 10^{17}/cm^3$ and $p = 9 \times 10^{17}/cm^3$, respectively. For contacts with non-linear characteristics the ρ_c-values for the forward direction are given. $I = 100$ mA corresponds to a current density of 560 A/cm^2

InP	Contact metal	Contact thickness/Å	Alloying time/min	Alloying temperature/°C	$\rho_c/\Omega cm^2$ for I = 1 mA	$\rho_c/\Omega cm^2$ for I = 100 mA	Remarks
n-type	Sn + Au	500 / 1200	5	400	1.2×10^{-4}	1.2×10^{-4}	linear; island formation
	In + Sn + Au	300 / 600 / 1200	2	400	3×10^{-4}	3×10^{-4}	linear; smooth surface
	Au/Ge + Ni	3000 / 700	2	300	1.7×10^{-3}	2.7×10^{-4}	non-linear
			2	350	1.2×10^{-6}	1.2×10^{-6}	linear; smooth surface; good adhesion
			2	400	1.2×10^{-6}	1.2×10^{-6}	
	Ni + Au/Ge + Ni	400 / 3000 / 700	2	350	4×10^{-6}	4×10^{-6}	
			1	400	2.3×10^{-6}	2.3×10^{-6}	
p-type	Au	1200	2	400	0.11	1.8×10^{-3}	strongly non-linear
			2	430	0.10	1.6×10^{-3}	
	Au/Ge	1600	2	400	1.8×10^{-2}	7.8×10^{-3}	slightly non-linear
	Cr + Au	800 / 1800	10	400	0.14	2.6×10^{-3}	strongly non-linear
	Zn + Au	700 / 1200	2	400	3.8×10^{-4}	3.8×10^{-4}	linear
			5	400	4.5×10^{-4}	4.5×10^{-4}	
	In + Zn + Au	300 / 900 / 1200	2	400	1.0×10^{-2}	8×10^{-4}	non-linear
			2	430	1.3×10^{-2}	8×10^{-4}	
	Au/Zn (99/1)	1400	2	430	7×10^{-2}	4×10^{-3}	non-linear; good adhesion
	Au/Zn (90/10)	1400	2	400	1.1×10^{-4}	1.1×10^{-4}	linear; good adhesion
			2	430	1.7×10^{-4}	1.7×10^{-4}	

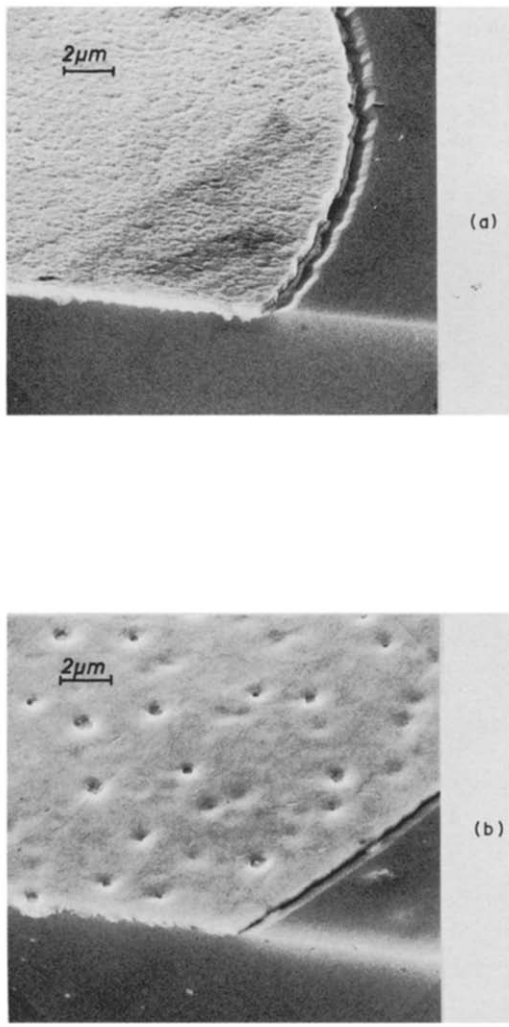

Fig. 3. SEM pictures of metal contacts on InP. A part of the layer surface as well as a cleaved edge of the contact is shown. The InP was etched by 0.2 μm in the contact area. (a) Au/Ge + Ni on n-InP alloyed at 400°C. (b) Au/Zn (90/10) on p-InP alloyed at 430°C.

R_m. Using the eqns (7) and (10), this condition can be written as

$$y \ll \frac{2}{\ln(4(s/d)-1)}. \quad (11)$$

In this study a modified four-point method was applied (see Fig. 1). The current I_{ad} is applied between points a and d, and the voltages U_{bc} between points b, c and U_{ab} between points a, b are measured. For the contact a, one finds

$$\rho_c = \frac{A}{I_{ad}}\left[U_{ab} - R_s - U_{bc}\frac{\ln((3s/d)-(1/2))}{2\ln 2}\right], \quad (12)$$

where R_s is given by eqn (8). Here, the current contacts and, therefore, the potential distribution remain fixed, whereas with the method of Ref. [23] the voltage contacts remain fixed. As a further advantage the series resistance contained in U_{ab} in eqn (12) is smaller than that in U'_{bc} in eqn (10), so that very small contact resistances can be more accurately determined.

4. RESULTS AND DISCUSSION

4.1 *Contacts to* n-*InP*

In Table 4 the properties of the contacts are summarized, which were found in this study. With contacts consisting of Sn + Au on n-InP, alloyed at 400°C, linear characteristics and a moderately low ρ_c-value were achieved. However, strong island formation occurred similar to that known for the Sn + Ag system[3]. With contacts consisting of In + Sn + Au, where In acted as a wetting agent, the resulting surface was smooth, but no lower ρ_c-values were achieved than with Sn + Au.

Very good contacts, however, were obtained with 3000 Å Au/Ge eutectic +700 Å Ni. While contacts alloyed at 300°C showed non-linear characteristics, the contacts alloyed at 350 and 400°C no longer revealed a deviation from linearity up to a current density >5 kA/cm². The characteristic is displayed in Fig. 2. With the combination Ni + Au/Ge + Ni no improvement was observed in the electrical data.

The specific contact resistance of Au/Ge + Ni on n-InP was as low as $1.2\times10^{-6}\,\Omega\text{cm}^2$. A comparison of this result with Table 3 shows that the type of current transport through these contacts is in the range between T–F-emission and pure field emission. The doping below the contact is then about $7\times10^{18}/\text{cm}^3$, provided that the model assumptions in Section 2 are justified.

The fact that our ρ_c-value is an order of magnitude lower than the one found by Erickson *et al.*[4] (see Table 1) is possibly due to the metallization thicknesses chosen here. The complex role, which the presence of Au and Ni plays during the incorporation of the Ge on donor sites, is discussed by Yoder[25].

The contacts showed a good adhesion property and a smooth surface, as shown in Fig. 3(a). Compared to the commonly used Au/Sn contacts, the combination used here offers the double advantage of a lower contact resistance and a higher mechanical stability.

4.2 *Contacts to* p-*InP*

Our results on contacts to p-InP are also presented in Table 4. Contacts made of pure Au show strongly non-linear characteristics after alloying. The same happens with Au/Ge evaporated as a eutectic and with Cr + Au. The latter result is in contrast to p-GaAs, where low resistance ohmic contacts are realized with Cr + Au. With p-InP, obviously only those metals provide ohmic contacts, which are known to be incorporated in epitaxial InP as acceptors such as Zn, Mg, Cd and Be. Good electrical results were obtained with contacts made of Zn + Au. However, the adhesion of Zn to InP is only moderate, so that thicker layers peeled off during the lift-off process. In order to improve the adhesion, a combination of In + Zn + Au was tried. However, the characteristic was non-linear. Contacts deposited from an Au/Zn alloy with 1 wt% Zn also resulted in non-linear characteristics.

The best contacts were achieved by evaporation of an

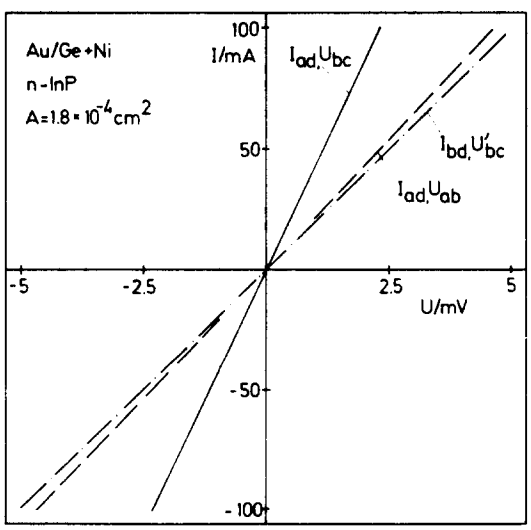

Fig. 2. Current–voltage characteristics of Au/Ge + Ni contacts on n-InP, alloyed at 400°C. The symbols are defined in Section 3.2.

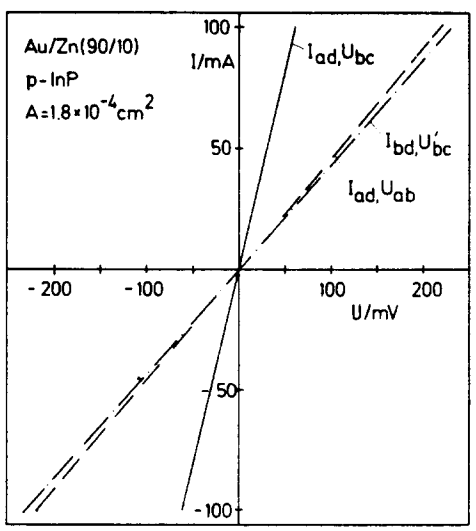

Fig. 4. Current–voltage characteristics of Au/Zn contacts on p-InP, alloyed at 430°C.

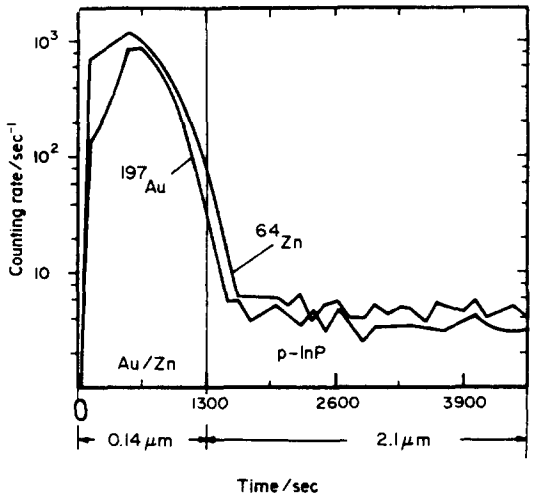

Fig. 5. Ion microprobe Au- and Zn-profile in arbitrary logarithmic units of an Au/Zn (90/10) contact on p-InP, alloyed at 430°C. The sputtering was done by 20 keV $^{32}O^+$-ions. Note the different sputter rate of 1.1 Å/s in the Au/Zn and 6.6 Å/s in the InP. The constant Zn- and Au-level in InP is background, e.g. due to redeposition.

Au/Zn alloy with 10 wt% Zn corresponding to the stoichiometric composition Au_3Zn. The current–voltage characteristics are extremely linear (see Fig. 4). The lowest specific contact resistance was $\rho_c = 1.1 \times 10^{-4}\ \Omega cm^2$ and was found after heat treatment at 400°C (see Table 4). The contact surface is relatively smooth, but submicron pinholes are visible, as shown in Fig. 3(b). The adhesion to InP is much better than with Zn + Au sequentially deposited. Moreover, the vacuum chamber is less contaminated with Zn by the evaporation of the Au/Zn alloy than by the separate evaporation of Zn + Au at two very different temperatures.

In order to examine the penetration depth of the fast diffusing Zn, the concentration profile of an alloyed Au/Zn contact was measured with an ion microprobe. As shown in Fig. 5, Zn does, however, not penetrate farther into the InP than Au does. The observed tail of Au and Zn, which is about 0.15 μm deep, presumably results from a mixing of liquid Au and Zn with the dissolved InP in the surface region. The diffusion of Zn into solid InP during 2 min at 430°C is obviously a minor effect. A comparison of the measured $\rho_c = 1.1 \times 10^{-4}\ \Omega cm^2$ with Table 3 shows that the type of current transport through these contacts is the field emission. The acceptor concentration corresponding to this ρ_c-value is $\sim 1 \times 10^{19}/cm^3$. Zn doping in LPE InP saturates at a hole concentration of $4 \times 10^{18}/cm^3$ [26, 27], whereas for Mg doping no saturation behaviour was found. On the other hand, the best ρ_c-value obtained so far with alloyed Au/Mg contacts on p-InP ($\sim 1 \times 10^{-4}\ \Omega cm^2$ [4]) is not lower than our ρ_c with Au/Zn contacts. This suggests that the relatively large contact resistance is not caused by the limited hole concentration achieved with Zn, but is mainly due to the high surface barrier of p-InP.

5. APPLICATION TO QUATERNARY LASERS

The described contacting technique using Au/Ge + Ni on n-InP and Au/Zn on p-InP was successfully applied to the preparation of $In_{1-x}Ga_xP_{1-y}As_y$/InP lasers emitting at $\lambda = 1.25\ \mu$m. The planar stripe lasers were proton-defined to have an active volume of $0.2 \times 8.5 \times 200\ \mu m^3$. At the threshold, which was as low as 140 mA, the voltage drop was 2.5 V. The differential resistance was 5 Ω in agreement with the above quoted ρ_c-values.

6. CONCLUSIONS

Ohmic contacts to n-InP and p-InP have been made which show the smallest contact resistances published so far. Furthermore, these contacts have good technological properties, which make them suitable for device applications, e.g. lasers. Comparison of the observed contact resistances with the theory of current transport through contacts allows the following conclusion: For n-InP, the low surface barrier combined with the high obtainable donor concentration by alloying enables the realization of extremely small ρ_c-values. For p-InP, the high surface barrier obviously inhibits the realization of $\rho_c < 10^{-4}\ \Omega cm^2$.

Acknowledgements—The author wishes to thank H. Feuerbach for technical assistance, and A. Pöcker and G. Lemm for performing the ion microprobe measurements.

REFERENCES

1. R. Becker, *Solid-St. Electron.* **16**, 1241 (1973).
2. G. Weimann and W. Schlapp, *Phys. Stat. Sol. (a)* **50**, K219 (1978).
3. H. T. Mills and H. L. Hartnagel, *Int. J. Electron.* **46**, 65 (1979).
4. L. P. Erickson, A. Waseem and G. Y. Robinson. *Thin Solid Films*, **64**, 421 (1979).
5. J. J. Hsieh, *Appl. Phys. Lett.* **28**, 283 (1976).
6. T. P. Pearsall, B. I. Miller, R. J. Capik and K. J. Bachmann, *Appl. Phys. Lett.* **28**, 499 (1976).
7. C. E. Hurwitz and J. J. Hsieh, *Appl. Phys. Lett.* **32**, 487 (1978).
8. T. P. Pearsall and M. Papuchon, *Appl. Phys. Lett.* **33**, 640 (1978).
9. T. Yamamoto, K. Sakai, S. Akiba and Y. Suematsu, *IEEE J. Quant. Electron* **QE-14**, 95 (1978).
10. L. M. Schiavone and A. A. Pritchard, *J. Appl. Phys.* **46**, 452 (1975).
11. F. A. Thiel, D. D. Bacon, E. Buehler and K. J. Bachmann, *J. Electrochem. Soc.* **124**, 317 (1977).
12. C. A. Mead, *Ohmic Contacts to Semiconductors* (Edited by B. Schwartz) p. 3. Electrochemical Soc. New York (1969).
13. G. Weimann, *Thin Solid Films*, **56**, 173 (1979).
14. A. M. White, A. J. Grant and B. Day, *Electron. Lett.* **14**, 409 (1978).
15. H. Nickel and E. Kuphal, (to be published).
16. D. Fritzsche, *Inst. Phys. Conf. Ser. No.* 50, 258 (1980).
17. V. L. Rideout, *Solid-St. Electron.* **18**, 541 (1975).
18. J. Vilms and L. Wandinger, *Ohmic Contacts to Semiconductors* (Edited by B. Schwarz) p. 31. Electrochem. Soc., New York (1969).
19. A. Y. C. Yu, *Solid-St. Electron.* **13**, 239 (1970).
20. P. Lawaetz, *Phys. Rev.* **B4**, 3460 (1971).
21. R. H. Cox and H. Strack, *Solid-St. Electron.* **10**, 1213 (1967).
22. W. Kellner, *Siemens Forsch.-u. Entwickl.-Ber.* **4**, 137 (1975).
23. L. E. Terry and R. W. Wilson, *Proc. IEEE* **57**, 1580 (1969).
24. Y. K. Fang, C. Y. Chang and Y. K. Su, *Solid-St. Electron.* **22**, 933 (1979).
25. M. N. Yoder, *Solid-St. Electron.* **23**, 117 (1980).
26. M. G. Astles, F. G. H. Smith and E. W. Williams, *J. Electrochem. Soc.* **120**, 1750 (1973).
27. E. Kuphal, *Techn. Ber.* 65 *TBr* 20 *des Forschungsinstitutes der DBP beim FTZ* (1979).